The structure of elongation factor G in complex with GDP: conformational flexibility and nucleotide exchange

Salam Al-Karadaghi[1], Arnthor Ævarsson[1], Maria Garber[2], Julia Zheltonosova[2] and Anders Liljas[1]*

Background: Elongation factor G (EF-G) catalyzes the translocation step of translation. During translocation EF-G passes through four main conformational states: the GDP complex, the nucleotide-free state, the GTP complex, and the GTPase conformation. The first two of these conformations have been previously investigated by crystallographic methods.

Results: The structure of EF-G·GDP has been refined at 2.4 Å resolution. Comparison with the nucleotide-free structure reveals that, upon GDP release, the phosphate-binding loop (P-loop) adopts a closed conformation. This affects the position of helix C_G, the switch II loop and domains II, IV and V. Asp83 has a conformation similar to the conformation of the corresponding residue in the EF-Tu/EF-Ts complex. The magnesium ion is absent in EF-G·GDP.

Conclusions: The results illustrate that conformational changes in the P-loop can be transmitted to other parts of the structure. A comparison of the structures of EF-G and EF-Tu suggests that EF-G, like EF-Tu, undergoes a transition with domain rearrangements. The conformation of EF-G·GDP around the nucleotide-binding site may be related to the mechanism of nucleotide exchange.

Addresses: [1]Department of Molecular Biophysics, Lund University, P.O. Box 124, S-221 00 Lund, Sweden and [2]Institute of Protein Research, Russian Academy of Sciences, 142292 Pushchino, Moscow region, Russia.

*Corresponding author.

Key words: antibiotic resistance, conformational transitions, elongation factor G, GTPases, protein synthesis

Received: 16 Jan 1996
Revisions requested: 5 Feb 1996
Revisions received: 8 Mar 1996
Accepted: 13 Mar 1996

Structure 15 May 1996, 4:555–565

Introduction

The bacterial peptide elongation factor G (EF-G) and its counterpart in Eucarya and Archaea, EF-2, belong to the GTPase superfamily of proteins. These proteins have a wide variety of functions in living cells [1]. The functional cycle of GTPases includes at least four major conformational states: the complex with GDP, the nucleotide-free (empty) state, the active GTP complex and the GTPase state [2]. EF-G, in complex with GTP, catalyzes the translocation step of translation. During translocation the peptidyl-tRNA is moved from the A site to the P site of the small subunit of the ribosome and the mRNA is shifted one codon relative to the ribosome [3]. When translocation has been completed GTP is hydrolyzed and EF-G dissociates from the ribosome [4]. The factor is reactivated by the subsequent substitution of GDP by GTP.

The three-dimensional structures of the GDP complex and the nucleotide-free form of EF-G, from *Thermus thermophilus*, have been determined to 2.7 Å and 2.85 Å resolution respectively [5,6]. The protein is composed of five domains. Domain I (the G domain) has a version of the nucleotide-binding fold similar to that found in other GTPases, like $p21^{ras}$, EF-Tu and transducin [7–10], while the topology of domain II is similar to the topology of domain II in EF-Tu. Recently, a structure-based analysis of sequence data revealed that domain II is present in all translation GTPases [11]. The fold of domain IV shows similarities to a fold within the ribosomal protein S5 [12,13], while domain V is related to ribosomal and RNA binding proteins (like S6 and U1A [14,15]). The fold of domain III is unclear due to crystal disorder, preventing unambiguous interpretation of the electron density map.

The transitions between the different conformational states of the GTPases are crucial for their function as molecular switches. In EF-Tu, GDP/GTP exchange is catalyzed by elongation factor Ts (EF-Ts), and leads to drastic spatial rearrangements of the position of domains II and III relative to the G domain [8,9,16]. This transition is triggered by a conformational change of the switch II region of the G domain in the vicinity of the nucleotide-binding site. Surprisingly, the spatial arrangement of domains I and II in the GTP complex (but not the GDP complex) of EF-Tu is similar to the arrangement of the respective domains both in the nucleotide-free form and the GDP complex of EF-G [5,6]. Moreover, the overall shape of EF-G is similar to the shape of the ternary complex of EF-Tu·guanosine 5′-[β,γ-imido] triphosphate (GDPNP)·aminoacyl(aa)tRNA [17], with domains III, IV and V of EF-G mimicking the tRNA. This observation is consistent with the existence of a common site for elongation factor binding on the ribosome [18].

The nucleotide-binding sites in all previously determined structures of GTPases are well conserved. Conservation extends to the interactions of the consensus sequence elements with the bound GDP/GTP and the magnesium ion.

However, a conserved residue (Lys25) within the phosphate-binding loop (P-loop) in EF-G, has a different conformation with its side chain rotated by about 180° around the Cα–Cβ bond and does not interact with GDP as in the other GTPase structures [5]. These differences may be related to the fact that EF-G lacks a guanine nucleotide exchange factor (GEF) and may possess an internal nucleotide exchange mechanism. A detailed comparison of the nucleotide-binding mode in EF-G and EF-Tu may shed some light on this mechanism.

In this paper we compare the structure of the EF-G·GDP complex, refined at 2.4 Å resolution, with the structure of the nucleotide-free form. Comparisons are also made with the structures of EF-Tu·GDP, EF-Tu·GDPNP and EF-Tu·EF-Ts. We show that the conformational change in the P-loop (residues 19–26) is propagated by a shift of helix C_G (residues 116–123) to the switch II region (residues 85–100) and to domains II, IV and V. The comparison has revealed the important role of both the P-loop and helix C_G of the G domain in the conformational transition following nucleotide release. The nucleotide-binding sites in EF-G and EF-Tu are compared in detail and the differences are discussed in terms of magnesium binding and nucleotide exchange.

Results

The three-dimensional structure of the EF-G·GDP complex has been refined to a crystallographic R factor of 22% at 2.4 Å resolution, using the structure of the empty factor as a starting model. The refined structure of the complex was used for additional refinement of the structure of the empty conformation and for resolving ambiguities in some loop regions.

The overall structure of EF-G (Fig. 1) has been described earlier [5,6]. Secondary structural elements were defined using the program DSSP [19] and by inspection of the hydrogen bonding network using computer graphics. In this work we follow the designation of secondary structural elements previously adopted [6]. The N-terminal domain is the nucleotide-binding domain (the G domain) with an insert consisting of residues 158–253 (the G′ subdomain). The other domains are numbered consecutively as they occur along the sequence (I–V). Strands and helices are denoted by numbers and capital letters respectively in order of their occurrence along the polypeptide chain within each domain. A subscript is added to each strand and helix designating its domain affiliation. Loops are described by the two secondary structural elements between which they occur.

Comparison of the nucleotide-free and GDP-bound structures

The dissociation of GDP from EF-G does not change the overall fold of the protein. Cα trace models of the nucleotide-free factor and the GDP complex after least-squares superposition of the Cα atoms of the G domains are shown in Figure 2. The root mean square (rms) value for the Cα atoms of the G domain is 0.83 Å. As seen from the figure there are some clear displacements of domains II, IV and V relative to the G domain. The rms deviation for the Cα atoms, after least-squares superposition of the G domains of the nucleotide-free and GDP complex structures, are 1.1 Å, 2.3 Å and 1.5 Å for domains II, IV, and V respectively. A major part of these differences can be described as a 3° rotation of domains II, IV, and V of the GDP structure relative to the G domain.

The hydrophilic nature of the surface between domains I and V will favour domain flexibility. The surface charge distribution and the limited area involved in this interdomain interaction (about 380 Å^2) can be seen in Figure 3. In total there are five arginine, one lysine and two glutamate residues close to the interface. The side chains of Glu119 and Arg123 make hydrogen bonds to the side chains of

Figure 1

A ribbon diagram of the overall three-dimensional structure of EF-G in complex with GDP. The numbers refer to the different domains. The bound GDP is shown as a ball-and-stick model.

Figure 2

A Cα trace model of the nucleotide-free (green) and the GDP complex (red) of EF-G after least-squares superposition of the Cα atoms of the G domains. The N terminus is labelled

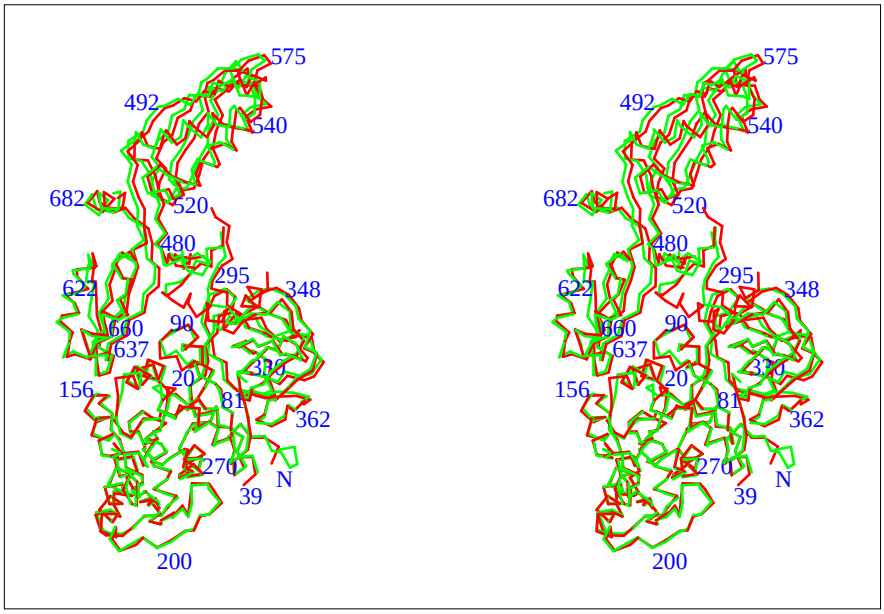

Arg666 and Asn639 respectively. Arg666 belongs to loop 2_5–3_5 and Asn639 to loop B_5–4_5. The polar character of the interactions makes this interface similar to the interface between domains I and III in EF-Tu in the GTP conformation. The rearrangement of the domains in EF-Tu upon the transition from the GTP to the GDP form disrupts these contacts and leads to the exposure of the interface to solvent [8,9].

The largest local differences between the empty form of EF-G and the EF-G·GDP complex are observed around the GTP/GDP binding site. Figure 4 shows these regions in both structures after a least-squares superposition of the G domains. They include the P-loop 1_G–A_G which has the consensus element Gly/Ala-x-x-x-x-Gly-Lys-Thr/Ser (residues 19–26), the switch II region including the consensus element Asp-x-x-Gly and helix B_G (residues 85–100), helix C_G (residues 117–123) and loops 4_G–C_G and C_G–5_G.

Similar differences were observed when we compared the EF-G·GDP structure, solved at Yale, to the nucleotide-free EF-G. However, there were some differences between the EF-G·GDP model we present and the Yale model. Probably the most prominent difference is in the position of Val88 and Asp89 within the switch II loop. In the Yale model the positions of these residues are shifted by about 7 Å from their positions in our model. In our maps there are some trace densities in the position of the Yale model main chain. These could be attributed to an alternative conformation of the loop, but no density which could be assigned to the side chains of Val88 and Asp89 could be located in that region.

Figure 3

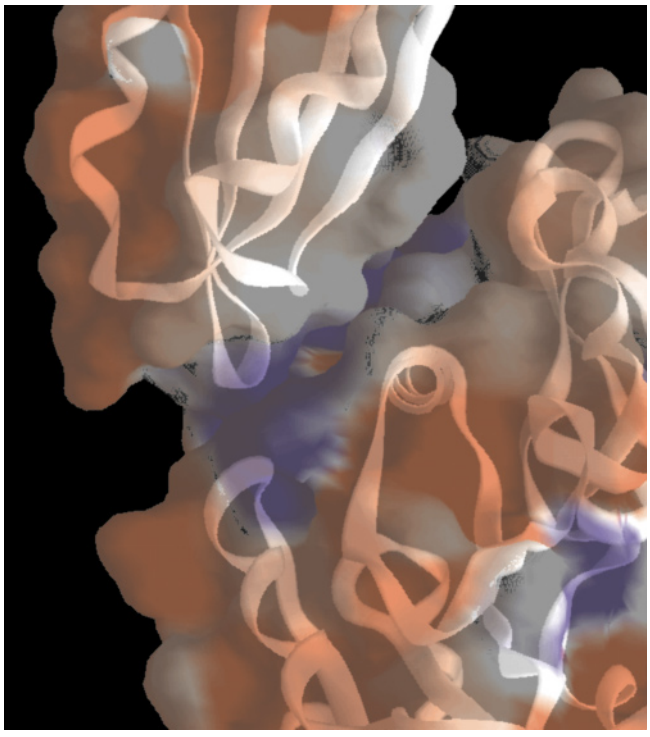

Surface electrostatic potential at the interface between the G domain (bottom) and domain V (top) of the EF-G·GDP complex. The surface is coloured from blue to red corresponding to the positive and negative potential respectively, with neutral points coloured white. Dark blue corresponds approximately to a potential greater than +6 kcal and red to a potential less than –4 kcal. (Figure generated with the program GRASP [42].)

Figure 4

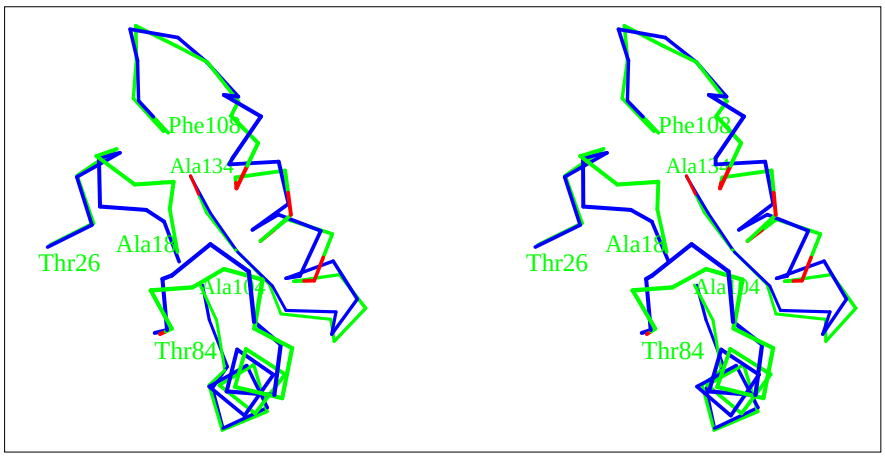

Stereo view of Cα traces of helix C_G, helix B_G, the switch loop (residues 84–104), and the phosphate-binding loop (residues 18–26) from the nucleotide-free EF-G structure (blue) and the EF-G·GDP complex (green) after a least-squares superposition of the respective G domains. The locations of fusidic acid resistant mutations are shown in red.

The conformation of the P-loop

Figure 5 presents the P-loop, helix C_G and the switch II loop after superposition of the Cα atoms of the G domain in the two conformations. Large displacements are observed for His20 and Ile21, with their Cα atoms shifted by about 2.8 Å and 2.5 Å respectively. In addition, the peptide plane between Ile21 and Asp22 is rotated by about 180°. The presence of GDP forces the loop to open up in order to accommodate the nucleotide. The carbonyl oxygen of Ile21 in the nucleotide-free enzyme occupies the position of the β phosphate of GDP. A nucleotide forces this carbonyl to a new position 5.4 Å away from that in the empty structure and 3.1 Å from Nδ1 of His20. This hydrogen bond replaces the bond between Oδ2 of Asp22 and Nδ1 of His20. A similar displacement of the P-loop, with associated peptide bond flip upon nucleotide binding, was observed in adenylate kinase [20] and F_1-ATPase [21]. However, in the case of adenylate kinase the loop movement is in the reverse direction: it closes in the presence of a phosphate and opens up in the nucleotide-free form.

The flip of the loop is accompanied by some rearrangement of the main chain atoms and the hydrogen bonding network. Thus, the hydrogen bond between the carbonyl of Ile21 and the amide of Gly24, which contributes to the stabilization of the loop in the nucleotide-free structure (3_{10}-type bond), is disrupted. The bond is shifted by one residue and replaced by a hydrogen bond between the corresponding groups of His20 and Ala23 in the EF-G·GDP complex. In the empty structure, the hydrogen bond from the carbonyl of Asp22 to Nδ1 of His20 replaces a bond to Nζ of Lys138 after the conformational change. A similar bond also occurs in both the GDP and the GDPNP complexes of EF-Tu (Asp21–Lys136 in *Escherichia coli*) [8,9].

The P-loop requires external interactions with the rest of the protein for stabilization of its conformation [22]. In the GDP complex the side chain of His20 is sandwiched between the negatively charged side chain of Glu115 and the polar Gln117. Despite the change in conformation the hydrogen bonding distance between His20 and Gln117 is

Figure 5

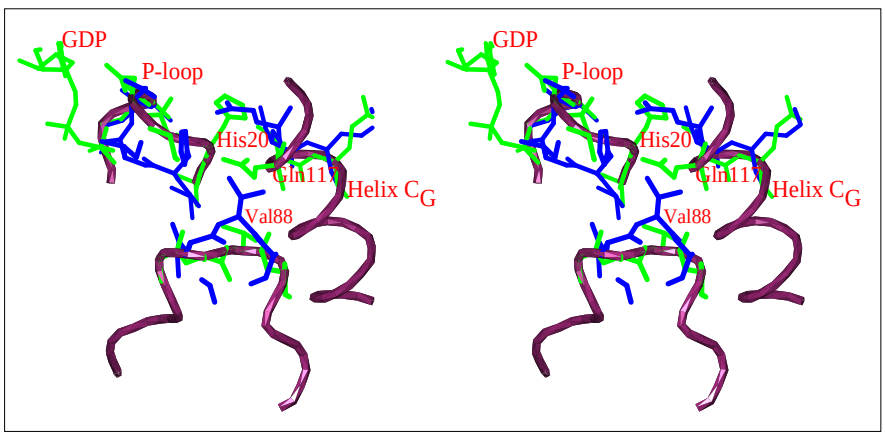

A least-squares superposition of the G domains of nucleotide-free EF-G and the EF-G·GDP complex showing side-chain interactions in the phosphate-binding loop, helix C_G and the switch II loop in the two structures. Residues from the empty structure are in blue and from the EF-G·GDP structure in green. His20 belongs to the P-loop, Gln117 to helix C_G and Val88 to the switch II loop.

maintained in both the empty and GDP-bound forms of the enzyme. These interactions may contribute to the stabilization of the conformation of the P-loop.

The shift of helix C_G

The displacement of His20 after nucleotide binding would bring the imidazole ring into close contact with the side chain of Gln117, which in turn has to move. This displacement triggers a shift of helix C_G relative to its position in the nucleotide-free structure. The shifts for the Cα atoms of Glu115, Pro116 and Gln117 between the empty structure and the GDP complex are about 2 Å, while for the rest of the residues in the helix the shift is about 1 Å. Helix C_G is packed against helix B_G on one side and against domain V on the other. Its location at the interface between domains I and V is of special interest since the shift of helix C_G, after nucleotide binding, may affect the position of domains V and IV.

The switch II region

The switch II region plays an important role in the transition from the GDP-bound to the GTP-bound conformation of GTPases [8,9,23]. In EF-Tu the γ phosphate of the nucleotide triggers drastic conformational changes around residues 83–96. During this transition the residues that form helix B are shifted, with some atoms having positional differences of up to about 8 Å between the GTP- and GDP-complex structures. In EF-G the differences between the GDP-bound and empty structures in this region are caused by the flip of the P-loop and the rigid body shift of helix C_G. These changes result in the side chain of Gln117 being brought into close contact with the side chain of Val88 (Fig. 5). As a consequence Cα and Cβ of this valine move by about 2.4 Å and 3.4 Å respectively. In contrast to the transition from EF-Tu·GTP to EF-Tu·GDP, the conformational transition of this loop in EF-G·GDP is of local character and does not lead to large domain rearrangements. Apart from Val88, only Gly86 and His87 are notably displaced (about 2.0 Å for the Cα atoms). Unfortunately, the electron density in this region, both in the empty state and in the GDP complex of EF-G, is rather poor and does not permit a more detailed analysis of the conformation.

GDP binding

The interactions of GDP with EF-G are shown schematically in Figure 6. The phosphates interact only with main chain atoms and solvent, while the guanine base interacts mainly with side chains.

The EF-G residues involved in interactions with GDP belong to the consensus sequence elements common to all GTPases. However, when compared to EF-Tu, p21*ras* and transducin there are significant differences from the corresponding interactions in EF-G. These differences were initially attributed to the absence of Mg^{2+} during crystallization [5]. One difference is the absence of the bond

Figure 6

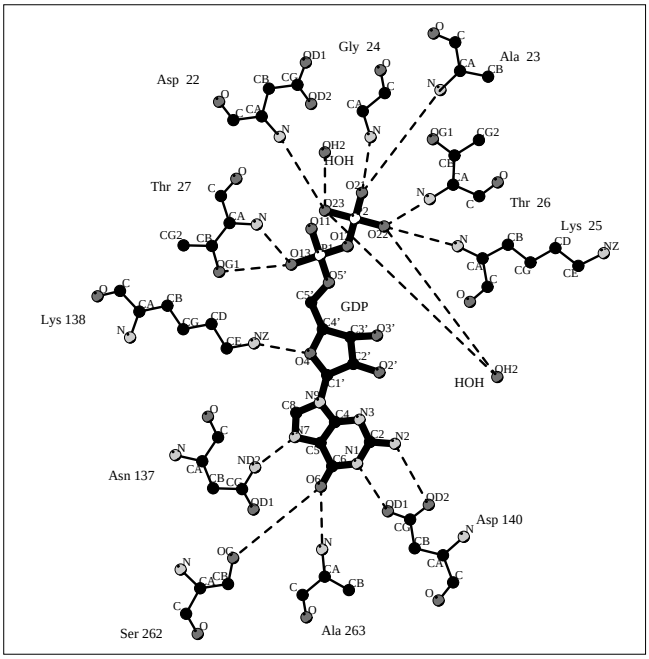

A schematic representation of the interactions of GDP with EF-G. The structure of GDP is shown with thick lines. Phosphorus atoms are depicted as open circles, nitrogens are lightly shaded and carbons and oxygens are black. Hydrogen bonds are shown by dashed lines. The figure was generated with the program LIGPLOT [43].

from Lys25 (in the P-loop) to the β phosphate of the nucleotide. This was considered to be one of the reasons for the higher observed affinity of GDP for EF-Tu than for EF-G (dissociation constant (K_d) 4.9×10^{-9} M and 1.1×10^{-5} M respectively for *E. coli* [4]).

In order to compare the interactions of the nucleotide with EF-G and EF-Tu the G domains of *E. coli* EF-Tu·GDP [24], *Thermus aquaticus* EF-Tu·GDPNP [9], *E. coli* EF-Tu·EF-Ts [16] and EF-G·GDP were superimposed using the least-squares superposition option of the program O [25]. The initial superposition included all the residues from the G core domain of EF-G (G′ excluded) and the G domain of EF-Tu and gave an rms deviation of 3.3 Å. The best fit was obtained for residues around 100–140 (EF-G numbering). Only these residues were included in the second round of refinement of the relative orientation and yielded an rms value of 0.64 Å. Figure 7 shows the P-loop, helix B_G and strand 3_G (residues 78–83) for EF-Tu·GDP, EF-Tu·GDPNP, EF-Tu·EF-Ts and EF-G·GDP. The most prominent feature of this figure is that strand 3_G (which proceeds the switch loop and helix B_G) is significantly displaced in EF-G, relative to the corresponding strands in both EF-Tu–nucleotide complexes, while in EF-Ts it occupies an intermediate position. This strand includes Asp83, a magnesium ligand known to be conserved in all GTPases and ATPases [22].

Figure 7

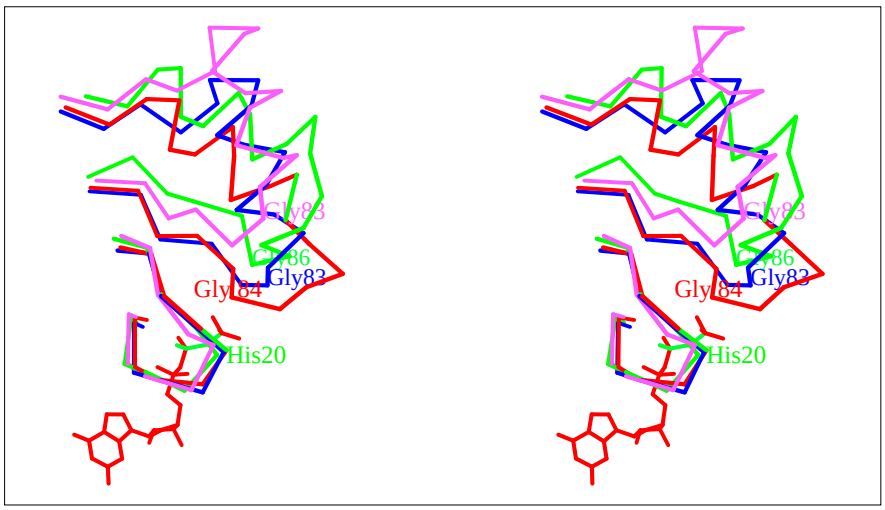

A comparison stereoview of the nucleotide-binding site in EF-Tu and EF-G. The P-loop and the switch II region are shown after least-squares superposition of the structures of EF-G·GDP (green), *E. coli* EF-Tu·GDP (blue), *T. aquaticus* EF-Tu·GTP (red) and *E. coli* EF-Tu·EF-Ts (pink). The GDP is shown in red at the bottom of the stereodiagram. For details of the superposition, see text.

Figure 8a shows the electron-density map of the residues around the magnesium-binding site. Figure 8b shows the consequences for magnesium coordination of the shift for strand 3_G in EF-G, relative to the respective strands in EF-Tu·GDP and EF-Tu·EF-Ts. In EF-G the shift of this strand (including Asp83) allows the rotation of the side chain of Lys25 (by about 180°) around the Cα–Cβ bond compared to the corresponding Lys24 in EF-Tu (*T. aquaticus* numbering). In this position the ζ amino group of Lys25 is at a hydrogen-bonding distance from Oδ1 of Asp83, almost coinciding with the position of the side chain of the homologous Asp81 from EF-Tu. The site corresponding to the ζ amino group of Lys24 of EF-Tu is occupied by a solvent molecule in the EF-G.GDP complex. As a result the bond from Lys25 to the β phosphate of GDP, present in other GTPase structures in complexes with GDP and with GTP analogues [8,10,23,24,26], is lost in EF-G. The intermediate position of strand 3_G in the EF-Tu·EF-Ts complex (between the corresponding strands in EF-G·GDP and EF-Tu·GDP) leads to a displacement of Asp80, Cys81 and Pro82. All of these residues are known ligands for water molecules that are involved in the coordination of the magnesium ion [16]. The side chain of Lys24 seems to follow the movement of

Figure 8

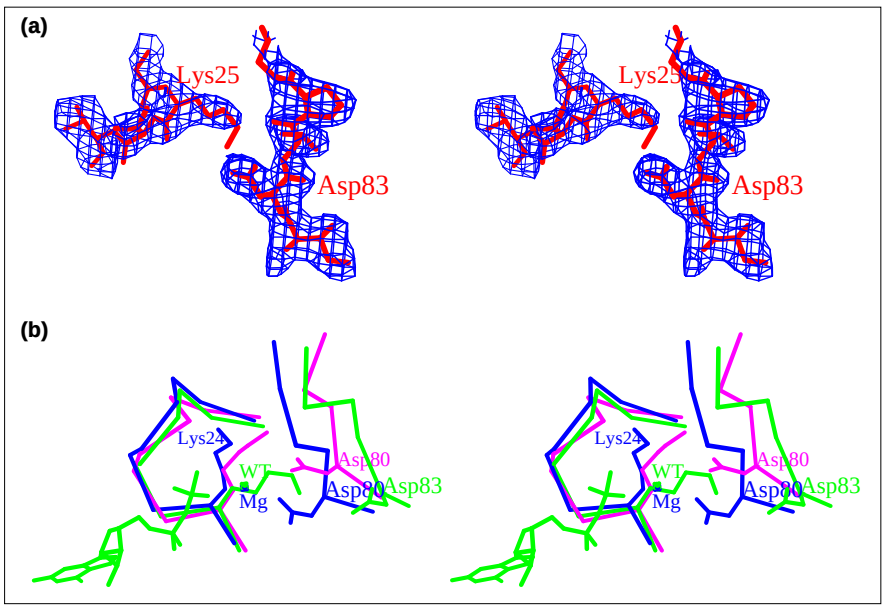

(a) The structure of EF-G·GDP around the magnesium-binding site superimposed on the electron density ($3F_o–2F_c$, contoured at 1σ level). (b) The differences in the location of strand 3_G and side chain conformations of Lys25 and Asp83 of EF-G·GDP (green), the corresponding Lys24 and Asp80 of EF-Tu·GDP (blue) and EF-Tu·EF-Ts (red). Green and blue crosses show the positions of a water molecule (WT) in EF-G·GDP and the magnesium ion (Mg) in EF-Tu·GDPNP respectively.

Figure 9

The location of Thr84 relative to Ile17 in EF-G·GDP (green) and after the superposition of strand 3_G of EF-G on the corresponding strand of EF-Tu (red and blue respectively).

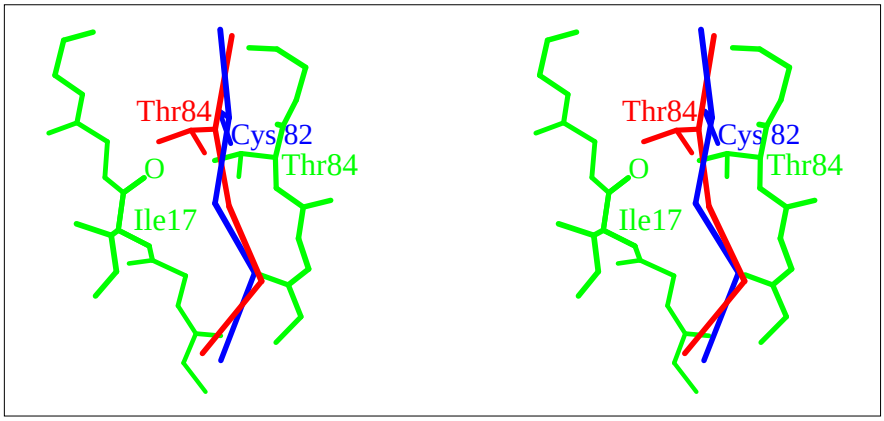

Asp80 and in its new position the Nζ atom is located 3.5 Å from the respective position in EF-Tu·GDP.

In the high-resolution, three-dimensional structures of p21*ras* and transducin complexes with GDP, the magnesium ion is coordinated to the β phosphate, to a conserved serine residue from the P-loop (threonine in EF-G and EF-Tu) and to solvent molecules with metal–ligand distances of around 2 Å, these distances are common to all known magnesium complexes [23,26,27]. Despite the presence of magnesium in our crystallization of the EF-G·GDP complex, the electron density found close to the magnesium-binding site was interpreted as a water molecule (Fig. 8b). It is positioned at about 3.5 Å and 4.2 Å from the β-phosphate oxygen and Thr26 respectively. The long distances to the ligands, the shift of Asp83 from its liganding position and the presence of the positively charged Lys25 group in the vicinity of the magnesium-binding site would argue against the presence of a magnesium ion at this position.

It is also interesting to compare the distances from the main chain amide group of Gly86, which belongs to the consensus sequence element Asp-x-x-Gly (Gly84 in *T. aquaticus* and Gly83 in *E. coli* EF-Tu), to the β phosphate of GDP. This residue plays a crucial role in the conformational change in EF-Tu. The flip of its peptide bond upon GTP binding brings its amide nitrogen into hydrogen bond distance of one of the γ-phosphate oxygen atoms and causes a change in the direction of helix B, which in turn affects the interactions between domains I and II and leads to the observed large domain rearrangements [8,9]. The Cα atom of Gly86 (from EF-G·GDP) is 2.2 Å and 5.0 Å from the corresponding residues in EF-Tu·GDP and EF-Tu·GDPNP respectively. The distance from the amide nitrogen to the β phosphate of the nucleotide is 10.2 Å, 8.0 Å and 6.2 Å in EF-G·GDP, EF-Tu·GDP and EF-Tu·GDPNP respectively. Assuming a similar mode of interactions of GTP with EF-G, a shift of about 4 Å is needed to bring this group into contact with the nucleotide.

Asp83 also needs to be shifted by almost the same distance (3.7 Å) to become a magnesium ligand. However, a shift of strand 3_G in the present conformation, to a position similar to that of the corresponding strand of EF-Tu, would be sterically hindered. The side chain of Thr84 would be approximately 1.5 Å from the carbonyl of Ile17 (strand 1_G, Fig. 9) and Lys25 would be 1 Å from Asp83. In other words, a substantial conformational rearrangement of this part of the G domain of EF-G may be needed to accommodate GTP. Thr84 is conserved in all known EF-G and EF-2 sequences. It is interesting that a double mutation, Thr88→Ala/Ala66→Val in *E. coli* EF-G (Thr84 and Ala68 in *T. thermophilus)*, results in reduced affinity for GTP and in resistance to the antibiotic fusidic acid [28]. In EF-Tu there is a cysteine residue at this position (Fig. 9). Its side chain conformation is different from the conformation of Thr84 in EF-G and does not lead to any unfavourable steric contacts.

Discussion

The conformation of the P-loop

The comparison of the structures of the nucleotide-free enzyme and the EF-G·GDP complex reveals several differences in conformation of the protein. The flip in the P-loop leads to displacements of helix C_G, the switch II region, helix B_G and domains II, IV and V. This transition demonstrates the mobility of these parts of EF-G relative to the G domain, this mobility may have functional relevance in the interaction of the factor with the ribosome. These differences in conformation can be regarded as part of the conformational transition which would be expected upon GTP binding. The flip of the P-loop may be a universal mechanism in mononucleotide binding proteins; in the case of EF-G it is used to trigger other conformational events through the interactions of His20 with Gln117.

The latter residue is intimately involved in transmitting the conformational changes to other parts of the protein. The crucial role of Gln117 in the dynamics of the protein is reflected in its conservation within other known EF-G and EF-*2* sequences.

Nucleotide exchange

The majority of GTPases interact with a nucleotide exchange factor (GEF) during their functional cycle to catalyse the GDP/GTP exchange. No such factor has been found for EF-G. In the case of *T. thermophilus* EF-Tu·GDP, the function of EF-Ts appears to be in raising the K_d for GDP from 1.1×10^{-9} M to 6.1×10^{-7} M, bringing it to a level close to that for GTP (5.8×10^{-8} M). The corresponding figures for EF-G are 1.1×10^{-5} M and 1.4×10^{-5} M for GDP and GTP respectively [4]. In other words, in EF-G, the K_ds for GDP and GTP are already similar; this could be a consequence of a built in mechanism for nucleotide exchange.

The molecular mechanism behind nucleotide exchange in EF-G remains unclear. The amino acids involved in nucleotide binding are amongst the most conserved in the family of mononucleotide binding proteins. Residues from the P-loop and from the consensus element Asp-x-x-Gly are responsible for triphosphate and magnesium binding, while the Asn-Lys-x-Asp element (residues 137–140 in EF-G) interacts with the guanine base. These interactions could be affected by nucleotide exchange factors either directly or indirectly.

The available structures of EF-G, EF-Tu and ATP synthase demonstrate analogous distortions upon nucleotide release. Thus, in all cases, a flip of a peptide bond in the P-loop is observed. In EF-Tu and ATP synthase nucleotide release leads to a shift of the strands corresponding to strands 1_G and 3_G in EF-G with an opening of the nucleotide binding site. The recently determined structure of the complex of EF-Tu·EF-Ts demonstrated that changes in the nucleotide-binding site that occur upon EF-Ts binding are similar to those observed in EF-G [16]. The strand containing Asp80, Cys81 and Pro82 (*E. coli* numbering) is displaced from its position in EF-Tu·GDP. These residues are involved in the stabilization of water molecules coordinating the magnesium ion. The displacement of this strand leads to the release of a magnesium ion, which appears to be necessary for nucleotide exchange. The shift in the position of strand 3_G of EF-G, relative to the position of the respective strand in EF-Tu, and the resulting new positions of Asp83 and Lys25 may be responsible for the absence of the magnesium ion in the EF-G·GDP complex and could be part of a built-in nucleotide exchange mechanism.

As discussed above Thr84 may play an important role in the observed separation of strands 1_G and 3_G in EF-G and thus in the transition from the GTP to the GDP conformation. In this respect, the fusidic acid resistant mutation Thr84→Ala (Thr88 in *E. coli* EF-G) is of special interest. The antibiotic fusidic acid blocks elongation by preventing the dissociation of the EF-G·GDP complex from the ribosome [4]. The presence of alanine instead of threonine would remove the steric constraints between strands 3_G and 1_G and may therefore allow Asp83 to bind the magnesium in the GDP form, leading to increased affinity for GDP. This would in turn affect the balance between the GTP and GDP states of the protein towards the GDP state. This may facilitate the dissociation of the factor from the ribosome. In contrast an alanine instead of a threonine may effectively interfere with nucleotide exchange and lead to reduced affinity for GTP [28].

The second group of interactions with the nucleotide, which are affected by EF-Ts, are those with the guanine base. A shift in the position of these residues would destabilize the binding of the guanine base [16]. In the case of EF-G there are extensive van der Waals' contacts between loop $2_{G'}$–$3_{G'}$ (residues 170–175) and loop 5_G–D_G (residues 137–145; which includes the consensus element Asn-Lys-x-Asp). In addition three hydrogen bonds from Oϵ of Glu171 to the amide of Gly143, from NH1 of Arg170 to the carbonyl of Ala144 and between the amide of Asp172 and the carbonyl of Asp140. A change in conformation of loop $2_{G'}$–$3_{G'}$ may disturb the interactions with the nucleotide and destabilize binding. Such flexibility could be facilitated by the two glycine residues (169 and 176) at the N and C termini of the loop. Both these residues are conserved in the EF-G/EF-*2* family. The G′ subdomain of EF-G (residues 158–253) has been suggested to serve as an internal nucleotide exchange factor for EF-G [5,6].

Fusidic acid resistant mutations and conformational flexibility

An analysis of fusidic acid resistant mutations has shown that they are clustered in three major regions in the central part of the protein [5,6,29]. One group is distributed in the G domain, the second group in domain III and the third group in domain V. The location of the mutations with respect to the observed conformational differences between the nucleotide-free structure and the GDP complex, points to several interesting aspects. As seen from Figure 4, four mutations (Thr84→Ala, Ala104→Glu, Tyr108→Ser and Ala134→Thr [29]) are found in the N- and C-terminal parts of the secondary structural elements. The largest conformational shifts, between the empty enzyme and GDP complexes of EF-G, occur within helix C_G and the switch II region. The mutations could therefore affect the conformational flexibility of these regions. Another group of mutations (Gln117→Arg, Thr120→Ile, Val121→Leu and Gln124→His) are localized in helix C_G. With the exception of Gln117 all mutated side chains face

helix B_G and the switch II region. A comparison of fusidic acid resistant mutations in EF-G with kirromycin resistant mutations in EF-Tu discloses some striking parallels. In EF-Tu there are three different substitutions of Gln124 (located at the end of helix C): Gln124→Arg, Gln124→Lys and Gln124→Glu (*E. coli* numbering) [30]. All these mutations add a new charge to the area, but whether the charge is negative or positive does not seem to be important. The new charge increases the polarity of the surface between domains I and III and probably leads to some destabilization of the interdomain contacts. This destabilization thus facilitates the transition to the GDP-bound conformation of the protein, which is necessary for its dissociation from the ribosome. In addition, it has been shown that the phosphorylation of Thr382, which is located close to the interface between domains I and III in EF-Tu, inhibits the formation of the ternary complex. This observation can be explained by a destabilization of the GTP form of EF-Tu necessary for complex formation [31].

Ribosome interactions

It was noted earlier that the conformation of the EF-G·GDP complex exhibits greater similarity to the conformation of the EF-Tu·GDPNP complex than to EF-Tu·GDP [3,18]. The ribosome is known to oscillate between two main conformational states (pre- and post-translational), with the two factors EF-Tu and EF-G catalyzing the transition between these states. Models which take into account conformational changes of the ribosome have been discussed earlier [32–34]. Since the binding sites for the elongation factors overlap, the ternary complex EF-Tu·GTP·aatRNA binds to the ribosome after the dissociation of EF-G·GDP, while EF-G·GTP binds after the dissociation of EF-Tu·GDP [3,18]. It is interesting that the overall shapes of the EF-G·GDP and EF-Tu·GDPNP·aatRNA structures are very similar [17]. Steric limitations imposed by the elongation factor binding site may require similarly shaped factors to interact with the same conformation of the ribosome. Thus, the conformational states of the factors and the ribosome would define their mutual affinity. It may be possible that the conformation of the EF-G·GTP complex is related to the open conformation of the EF-Tu·GDP complex, with major domain rearrangements. This idea is supported by the similar location of the kirromycin and fusidic acid resistant mutations within the three-dimensional structures of EF-Tu and EF-G respectively.

Biological implications

The elongation cycle of protein synthesis involves a number of steps: aminoacyl-tRNA binding to the ribosome catalyzed by EF-Tu·GTP, peptidyl transfer catalyzed by the ribosome, and translocation catalyzed by EF-G·GTP. After GTP hydrolysis the elongation factors dissociate from the ribosome. GTP hydrolysis leads to a large conformational change of EF-Tu·GTP with major domain rearrangements leading to the release of aatRNA and dissociation of EF-Tu from the ribosome [8,9].

Only the conformations of the nucleotide-free and GDP complex of EF-G are known. The comparison of these two structures in this work shows that the release of GDP leads to a flip of the P-loop, which affects the structures of helix C_G and the switch II region. Domains II, IV and V undergo a rigid body shift relative to the G domain. These differences reveal a certain amount of conformational flexibility of the protein and can be regarded as part of the conformational transition expected upon GTP binding. The similar locations of mutations leading to fusidic acid and kirromycin resistance in EF-G and EF-Tu, at the polar interfaces between the G domain and domains V and III respectively, suggests that this conformational transition may be similar in character to the transition observed in EF-Tu.

A comparison of the structure of the nucleotide-binding site of EF-G·GDP with the respective sites in EF-Tu, $p21^{ras}$ and transducin reveals that the conserved Lys25 from the P-loop and Asp83 from the GTPase consensus element (Asp-x-x-Gly) have notably different conformations. The shift of the strand containing Asp83 is similar in character to the shift observed for the respective strand in the EF-Tu·EF-Ts complex and accounts for the absence of the magnesium ion in EF-G·GDP. These conformational changes, which lead to an opening of the nucleotide-binding site, may be regarded as part of the GDP/GTP exchange mechanism common to all GTPases.

Materials and methods

EF-G from *T. thermophilus* was purified and crystallized using the hanging drop technique as described earlier [35], with some minor modifications to the crystallization procedure [36]. Magnesium sulphate was present at a concentration of 3 mM. Before transfer to glass capillaries for data collection the crystals were cross-linked with glutaraldehyde. The crystals of the GDP complex of the protein belong to space group $P2_12_12_1$ with cell dimensions a=76.3 Å, b=106.4 Å, c=115.6 Å (compared to a=75.6 Å, b=106.0 Å, c=116,4 Å for the nucleotide-free form). Synchrotron data were collected at beamline 9.6 in the Daresbury Laboratory using an MAR detector (wave length 0.87 Å). Due to their short life time in the beam, three crystals were used for data collection. An oscillation range of 1.25° was used. A total of 284 145 reflections were measured of which 32 595 were unique in the resolution range 10.0–2.4 Å (completeness 87%). The data were processed using the program DENZO (Z Otwinowski and W Minor, unpublished program) and scaled using SCALA [37]. The redundancy of the data was 4.2, R_{merge} 0.07. In the highest resolution shell completeness was 46% and R_{merge} 0.26% with $I/\sigma(I)$ of 2.9. Of the unique reflections 75.9% had $I > 3\sigma$.

Refinement

The refinement was carried out using the program X-PLOR [38] with the coordinates of the nucleotide-free protein as a starting model. After some cycles of rigid body refinement of the orientations and positions of the whole molecule and the domains, alternating cycles of simulated annealing, positional refinement and model building were employed. The model was checked visually and rebuilt using the graphics program O [25]. Simulated annealing omit maps [39] were used for

rebuilding regions with conformations different from those of the starting model. Potential solvent sites were identified using the peak search option in MAPMAN (GJ Kleywegt and TA Jones, unpublished program). The assignment of water molecules to the predicted sites was based on several criteria: the shape of the electron density, hydrogen-bonding possibilities and distance from neighbouring protein atoms and other solvent molecules.

Despite the higher resolution of the data, the electron density for domain III (residues 400–477) and the so-called effector loop (residues 38–67) was still weak and did not permit any reliable model building. Even data collected at –150°C did not lead to improvements in the electron-density maps in these regions (unpublished data). Some parts of domain III, for which the main chain density could be trace, were built as polyalanine chains.

The R-factor of the final model is 0.22% with an R-free of 29% in the resolution range 8.0–2.4 Å. It should be noted that these values are affected by the large disordered parts of the structure (domain III and the effector loop); only 614 protein residues (30 being modelled as alanine) out of 691 and 138 solvent molecules were included in the model. Rms deviations from ideality for bond lengths, bond angles and torsion angles are 0.014 Å, 1.97° and 26.29° respectively.

About 98% of main chain torsion angles have values inside the allowed region of the plot, with 85.3% falling into the core region (program PROCHECK [40]). Three residues were found in the high energy region of the plot. These were located on the surface of the protein and had poor electron density. The estimated coordinate error from the σ_a plot (not shown) is 0.53 Å [41].

The structure of the nucleotide-free form of the enzyme, for which data are available at 2.8 Å resolution [6], was further refined using the 2.4 Å model of the GDP complex as a guide for rebuilding some loop regions and side chains with ambiguous conformations. However, this did not lead to any changes in the overall structure of the model. The present R-factor for this model is 23% (R-free 32%) in the resolution range 8.0–2.8 Å, with rms deviations from ideality for bond lengths of 0.020 Å, for bond angles of 2.45° and for torsion angles of 26.60°.

Structures of the nucleotide-free EF-G and the GDP complex have been deposited with the Brookhaven Protein Data Bank.

Acknowledgements

The authors are grateful to the staff of the Daresbury Laboratory for assistance during data collection, to A Leslie for providing the coordinates of ATP synthase, to J Nyborg and co-workers for providing the coordinates of the GDP, GDPNP and GDPNP·aatRNA complexes of EF-Tu, and to T Kawashima for providing the coordinates of the EF-Tu·EF-Ts complex. This project has been supported by the Swedish Natural Science Research Council, the Russian Foundation for Fundamental Investigations (93–04–21151), the Royal Swedish Academy of Science, the Russian Academy of Sciences and NUTEK. The research of M. Garber has been partially supported by an International Research Scholar's award from the Howard Hughes Medical Institute.

References

1. Bourne, H.R., Sanders, D.A. & McCormick, F. (1991). The GTPase superfamily: conserved structure and molecular mechanism. *Nature* **349**, 117–127.
2. Liljas, A. (1990). Some structural aspects of elongation. In *The ribosome: structure, function & evolution.* (Hill, W.E., Dahlberg, A., Garrett, R.A., Moore, P.B., Schlessinger, D. & Warner, J.R., eds), pp. 309–317, American Society of Microbiology, Washington DC.
3. Spirin, A.S. (1985). Ribosomal translocation: facts and models. *Prog. Nucleic Acids Res. Mol. Biol.* **32**, 75–114.
4. Kaziro, Y. (1978). The role of guanosine 5′-triphosphate in polypeptide chain elongation. *Biochim. Biophys. Acta* **505**, 95–127.
5. Czworkowski, J., Wang, J., Steitz, T.A. & Moore, P.B. (1994). The crystal structure of elongation factor G complexed with GDP, at 2.7 angstrom resolution. *EMBO J.* **13**, 3661–3668.
6. Ævarsson, A., *et al*., & Liljas, A. (1994). Three-dimensional structure of the ribosomal translocase: elongation factor G from *Thermus thermophilus*. *EMBO J.* **13**, 3669–3677.
7. Pai, E.F., Kabsch, W., Krengel, U., Holmes, K.C., John, J. & Wittinghofer, A. (1989). Structure of the guanine-nucleotide-binding domain of the Ha-*ras* oncogene product p21 in the triphosphate conformation. *Nature* **341**, 209–214.
8. Berchtold, H., Reshetnikova, L., Reiser, C.O.A., Schirmer, N.K., Sprinzl, M., & Hilgenfeld, R. (1993). Crystal structure of active elongation factor Tu reveals major domain rearrangements. *Nature* **365**, 126–132.
9. Kjeldgaard, M., Nissen, P., Thirup, S. & Nyborg, J. (1993). The crystal structure of elongation factor EF-Tu from *Thermus Aquaticus* in the GTP conformation. *Structure* **1**, 35–50.
10. Noel, J.P., Hamm, H.E. & Sigler, P.B. (1993). The 2.2 Å crystal structure of transducin-α complexed with GTPγS. *Nature* **366**, 654–662.
11. Ævarsson, A. (1995). Structure-based sequence alignment of elongation factors Tu and G with related GTPases involved in translation. *J. Mol. Evol.* **41**, 1096–1104.
12. Murzin, A.G. (1995). A ribosomal protein module in EF-G and DNA gyrase. *Nat. Struct. Biol.* **2**, 25–26.
13. Ramakrishnan, V. & White, S.W. (1992). The structure of ribosomal protein-S5 reveals sites of interaction with 16S rRNA. *Nature* **358**, 768–771.
14. Lindahl, M., *et al*., & Amons, R. (1994). Crystal structure of the ribosomal protein S6 from *Thermus thermophilus*. *EMBO J.* **13**, 1249–1254.
15. Nagai, K., Oubridge, C., Jessen, T.H., Li, J. & Evans, P.R. (1990). Crystal structure of the RNA-binding domain of the U1 small nuclear ribonucleoprotein A. *Nature* **348**, 515–520.
16. Kawashima, T., Berthet-Colominas, C., Cusack, S., Wulff, M. & Leberman, R. (1996). The crystal structure of the *Escherichia coli* EF-Tu·EF-Ts complex at 2.5 Å resolution: mechanism of GDP/GTP exchange. *Nature* **379**, 511–518.
17. Nissen, P., *et al*., & Nyborg, J. (1995). Crystal structure of the ternary complex of the PhetRNA, elongation factor Tu and a GTP analogue. *Science* **270**, 1464–1472.
18. Liljas, A. (1982). Structural studies of ribosomes. *Prog. Biophys. Mol. Biol.* **40**, 161–228.
19. Kabsch, W. & Sander, C. (1983). Dictionary of protein secondary structure: pattern recognition of hydrogen-bonded and geometrical feature. *Biopolymers* **22**, 2577–2637.
20. Dreusicke, D. & Schultz, G.E. (1988). The switch between two conformations of adenylate kinase. *J. Mol. Biol.* **203**, 1021–1028.
21. Abrahams, J.P., Leslie, A.G.W., Lutter, R. & Walker, J.E. (1994). Structure at 2.8 Å resolution of F1-ATPase from bovine heart mitochondria. *Nature* **370**, 621–628.
22. Cronet, P., Bellsolell, L., Sander, C., Coll, M., & Serrano, L. (1995). Investigating the structural determinants of the p21-like triphosphate and Mg^{2+} binding site. *J. Mol. Biol.* **249**, 654–664.
23. Milburn, M.V., *et al*., & Kim, S.-H. (1990). Molecular switch for signal transduction: structural differences between active and inactive forms of protooncogenic *ras* proteins. *Science* **247**, 939–945.
24. Kjeldgaard, M. & Nyborg, J. (1992). Refined structure of elongation factor-EF-Tu from *Escherichia coli*. *J. Mol. Biol.* **223**, 721–742.
25. Jones, T.A., Zou, J,-Y., Cowan, S.W. & Kjeldgaard, M. (1991). Improved methods for building protein models in electron-density maps and the location of errors in these models. *Acta Crystallogr. A* **47**, 110–119.
26. Lambright, D.G., Noel, J.P., Hamm, H.E. & Sigler, P.B. (1994). Structural determinants for activation of the alpha-subunit of a heterotrimeric G protein. *Nature* **369**, 621–628.
27. Frausto da Silva, J.J.R. & Williams, R.J.P. (1991). In *The biological chemistry of the elements.* Monograph, Clarendon Press, Oxford.
28. Richter Dalfors, A. & Kurland, C.G. (1990). Novel mutants of elongation factor G. *J. Mol. Biol.* **215**, 549–557.
29. Johanson, U. & Hughes, D. (1994). Fusidic acid-resistant mutants define three regions in elongation factor G of *Salmonella typhimurium. Gene* **143**, 55–59.
30. Abdulkarim, F., Liljas, L. & Hughes, D. (1994). Mutations to kirromycin resistance occur in the interface of domains I and III of EF-Tu·GTP *FEBS Lett.* **352**, 118–122.
31. Alexander, C., *et al*., & Lippmann, C. (1995). Phosphorylation of elongation factor Tu prevents ternary complex formation. *J. Biol. Chem.* **270**, 14541–14547.
32. Spirin, A.S. (1969). A model of the functioning ribosome: locking and unlocking of the ribosome subparticles. *Cold Spring Harbor Symp. Quant. Biol.* **34**, 197–207.

33. Möller, W. (1974) . The ribosomal components involved in EF-G and EF-Tu- dependent GTP hydrolysis. In *Ribosomes.* (Nomura, M., Tissiéres, A., & Lengyel, P., eds), pp. 711–731, Cold Spring Harbor Laboratory, NY.
34. Mesters, J.R., Potapov, A.P., Degraaf, J.M. & Kraal, B. (1994). Synergism between the GTPase activities of EF-Tu·GTP and EF-G·GTP on empty ribosomes – elongation factors as stimulators of the ribosomal oscillation between two conformations. *J. Mol. Biol.* 242, 644–654.
35. Reshetnikova, L.S. & Garber, M.B. (1983). Crystallization of elongation factor G from an extreme thermophile, *Thermus thermophilus* HB8. *FEBS Lett.* 154, 149–150.
36. Garber, M., *et al*., & Al-Karadaghi S., (1996). Crystallization and structural studies of components of the protein synthesizing system from *Thermus thermophilus*. *J. Cryst. Growth*, in press.
37. Collaborative Computational Project, Number 4. (1994). The CCP4 suite: programs for protein crystallography. *Acta Cryst. D* 50, 760–763.
38. Brünger, A.T. (1990). *X-PLOR version 3.1, a system for X-ray crystallography and NMR.* Yale University Press, New Haven, CT.
39. Hodel, A., Kim, S.-H. & Brunger, A.T. (1992). Model bias in macromoleculer structures. *Acta Cryst. A* 48, 851-858.
40. Laskowski, R.A., MacArthur, M.W., Moss, D.S. & Thornton, J.M. (1993). PROCHECK: a program to check the stereochemical quality of protein structure coordinates. *J. Appl. Cryst*. 26, 283–291.
41. Read, R.J. (1986). Improved Fourier coefficients for maps using phases from partial structures with errors. *Acta Cryst. A* 42, 140–149.
42. Nicholls, A., Sharp, K. & Honig, B. (1991). Protein folding and association: insights from the interfacial and thermodynamic properties of hydrocarbons. *Proteins* 11, 281–296.
43. Wallace, A.C., Laskowski, R.A. & Thornton, J.M. (1995). LIGPLOT: a program to generate schematic diagrams of protein–ligand interactions. *Protein Eng.* 8, 143–146.